

## Molecular-dynamics study of the dynamic structure factors of molten LiCl and LiCl-CsCl

Susumu Okazaki, Yasushi Miyamoto, and Isao Okada

*Department of Electronic Chemistry, Tokyo Institute of Technology, 4259 Nagatsuta, Midori-ku, Yokohama 227, Japan*

(Received 2 July 1991)

The collective dynamics of ions in pure LiCl and LiCl-CsCl mixture melts has been investigated by use of molecular-dynamics calculations. Special attention was focused on the Brillouin peaks in variously defined dynamic structure factors  $S(k, \omega)$ . Phonon propagation was observed both in charge-charge and mass-mass density fluctuations in the melts, the former showing an optic-type dispersion curve and the latter an acoustic one. In particular, for the charge-charge density fluctuation, two different types of phonon modes certainly exist in the pure LiCl melt, and three in the LiCl-CsCl mixture melt; these modes are presumably based on more than one kind of state of the ionic motion in the melts. This phenomenon seems to be caused by a combination of the constituent small, light ions with the large, heavy ones in the melts.

### I. INTRODUCTION

Molecular-dynamics (MD) simulation, together with inelastic-neutron-scattering measurement, has been one of the most useful tools in the investigation of collective dynamics in classical liquids. One of the most interesting findings is that phonon wave propagation, which is widely observed in crystals, also exists even in the disordered liquid phase. In these studies, variously defined dynamic structure factors  $S(k, \omega)$  as well as power spectra of longitudinal and transverse current fluctuations have been examined in detail. In particular, interest has been focused on a Brillouin peak at nonzero frequencies in  $S(k, \omega)$ . For liquids of neutral particles, for example, a number of MD calculations,<sup>1-8</sup> inelastic-neutron-scattering measurements,<sup>9-12</sup> and theoretical studies<sup>13,14</sup> have been carried out, in which a Brillouin peak showing an acoustic dispersion relation was observed in all except one single case, that of inert-gas-particle liquids.<sup>7,12</sup>

Ionic liquids are more interesting. After the publication of the MD work on one-component plasmas by Hansen, McDonald, and Pollock<sup>15</sup> various investigations have been performed on molten salts composed of positive and negative ions, including MD calculations<sup>16-20</sup> and inelastic neutron diffraction.<sup>21-27</sup> Studies on solid electrolytes<sup>28,29</sup> may properly be considered to belong to the same category of these investigations. The findings of these studies on molten salts can be summarized as follows: (i) MD results of the dynamic structure factors as defined by the charge-charge and mass-mass density correlation functions [ $S_{CC}(k, \omega)$  and  $S_{MM}(k, \omega)$ , respectively, the basis functions of the ideal coupled oscillations] show that  $S_{CC}(k, \omega)$  has a distinct Brillouin peak with an optic dispersion relation, although the latter does not present such a peak<sup>16-18,20</sup> except for SrCl<sub>2</sub> in which an acoustic dispersion curve was observed.<sup>19</sup> (ii) Total neutron weighted dynamic structure factors  $S_T(k, \omega)$  obtained from the inelastic-neutron-scattering measurement do not show a Brillouin peak but only one quasielastic peak at  $\omega=0$  cm<sup>-1</sup> over the  $k$  range accessible to the ex-

periments. (iii) Based on the isotopic substitution method, the experimental total dynamic structure factors can be, in principle, decomposed into partial dynamic structure factors similar to the above  $S_{CC}(k, \omega)$  and  $S_{MM}(k, \omega)$ . Each of the corresponding neutron weighted power spectra of longitudinal current fluctuation  $C_{CC}(k, \omega)$  and  $C_{MM}(k, \omega)$ —instead of  $S_{CC}(k, \omega)$  and  $S_{MM}(k, \omega)$ —was examined and found to have a Brillouin peak, with somewhat complicated dispersion relations. (iv) All the Brillouin peaks observed so far are single, which indicates that there is only one single collective mode in the melts.

However, the total number of these investigations is rather small: To our knowledge, only four MD investigations for molten salts, i.e., for NaI, RbBr, NaCl, and SrCl<sub>2</sub>, have been reported. Thus, the above summary may be based on no more than one limited aspect of the collective dynamics of ionic liquids. Hence, fundamental studies must be applied to other salts to understand the collective properties of these liquids.

The most important and basic physical quantity that affects the ion dynamics is the mass of the ions and the interionic interaction. In the present study, interest was focused on the Li<sup>+</sup> ion, which is the lightest as well as the smallest metal ion, the smallest dimension causing the strongest interaction with counter anions. However, the MD ionic systems reported so far consist of relatively large, heavy cations and anions, while one of the present systems (pure LiCl) is composed of small, light Li<sup>+</sup> ions and large, heavy Cl<sup>-</sup> ions and another (LiCl-CsCl) has the considerably heavier and larger Cs<sup>+</sup> ions in addition to the other two. In both systems, the Li<sup>+</sup> ions were found in the interstitial region between the skeleton structure formed by the Cl<sup>-</sup> ions, the space being larger in the case of the LiCl-CsCl mixture than in the pure LiCl melt. In such liquids, the lighter and smaller ions have shown remarkable one-particle dynamics with oscillating character.<sup>30,31</sup> It is thus interesting to study the collective motions, i.e., propagation of phonons, in liquids that include small, light cations surrounded by

large, heavy counteranions.

For pure LiCl melt, an inelastic-neutron-scattering measurement was reported by Pusztai and McGreevy,<sup>27</sup> in which the isotopic substitution method was used to decompose spectra of the total longitudinal current correlation function  $C_T(k, \omega)$  to the partial ones,  $C_{CC}(k, \omega)$  and  $C_{MM}(k, \omega)$ . However, there was little discussion of the corresponding partial structure factors  $S_{CC}(k, \omega)$  and  $S_{MM}(k, \omega)$ , which are more interesting and informative. Furthermore, owing to experimental restrictions, their  $(k, \omega)$  space is so limited that a clear discussion of the dispersion relation was difficult. In the present study, very long MD runs for both pure LiCl melt and LiCl-CsCl mixture melt were performed to obtain sufficient data for greater precision of the calculated dynamic structure factors. Our  $(k, \omega)$  region was wider than that used by McGreevy and co-workers; in particular,  $S(k, \omega)$  at high frequencies  $\omega$  and at small wave numbers  $k$  was examined.

After the following brief description of the MD calculations, definitions of the calculated standard statistical mechanical functions, which represent dynamics in collective modes, are presented. In Sec. III, one-particle dynamics of  $\text{Li}^+$  ions as well as the collective motions of the melts is reported.

## II. CALCULATIONS

Molecular-dynamics simulations were performed for pure LiCl and LiCl-CsCl mixture melts. There were 256  $\text{Li}^+$  and 256  $\text{Cl}^-$  ions in the cubic cell for the pure salt and 26  $\text{Li}^+$ , 230  $\text{Cs}^+$ , and 256  $\text{Cl}^-$  ions for the mixture, the concentration of LiCl in the latter being approximately 10 mol %. In each system, the cell edge length  $L$  was evaluated from the experimental density,<sup>32</sup> i.e., 23.11 Å and 29.13 Å, respectively. The interionic potentials used were of the usual Born-Huggins-Mayer form. The potential parameters given by Tosi and Fumi<sup>33</sup> and by Dixon and Gillan<sup>34</sup> were adopted for LiCl and CsCl systems, respectively. The cross parameters for the mixture were determined using the combining rule proposed by Larsen, Førlund, and Singer.<sup>35</sup> Coulombic forces were computed by the Ewald method. The equation of motion was numerically integrated by the predictor-corrector algorithm with the *NEV* ensemble under periodic boundary conditions. The time step was chosen to be 2 fs, which provided sufficient conservation of the total energy through the present long MD runs. After the system reached equilibrium, runs of  $1.4 \times 10^5$  and  $2.4 \times 10^5$  MD steps, corresponding to 280 ps and 480 ps, were carried out for the pure and mixture melts, respectively, which gave satisfactory statistics for evaluation of various collective functions. The mean temperatures of the pure and mixture melts were 956 K and 963 K, respectively. This enables us to compare the calculated neutron weighted total static structure factor with the experimental one recently measured by us at 973 K, which will appear in a separate paper.

As usual, Fourier transformation of the fluctuating density of ions of species  $\alpha$  is given by

$$\rho_\alpha(\mathbf{k}, t) = \sum_j \exp[i\mathbf{k} \cdot \mathbf{r}_j(t)] , \quad (1)$$

where  $\mathbf{r}_j(t)$  denotes the position of the ion  $j$  at time  $t$  and the summation was performed only over the species  $\alpha$ . The total densities of charge and mass can then be expressed in terms of the partial density as

$$\rho_C(\mathbf{k}, t) = \sum_\alpha z_\alpha \rho_\alpha(\mathbf{k}, t) , \quad (2)$$

$$\rho_M(\mathbf{k}, t) = \sum_\alpha m_\alpha \rho_\alpha(\mathbf{k}, t) , \quad (3)$$

where  $z_\alpha$  and  $m_\alpha$  are the charge and mass of ions of species  $\alpha$ , respectively. The time correlation function of  $\rho_\alpha(\mathbf{k}, t)$  represents an intermediate partial structure factor  $F(k, t)$ ; for example, for a Li-Li pair

$$F_{\text{LiLi}}(\mathbf{k}, t) = N_{\text{Li}}^{-1} \langle \rho_{\text{Li}}(\mathbf{k}, t) \rho_{\text{Li}}(-\mathbf{k}, 0) \rangle . \quad (4)$$

In a similar way, autocorrelation functions for the fluctuating charge and mass densities are represented by

$$F_{CC}(\mathbf{k}, t) = N^{-1} \langle \rho_C(\mathbf{k}, t) \rho_C(-\mathbf{k}, 0) \rangle , \quad (5)$$

$$F_{MM}(\mathbf{k}, t) = N^{-1} \langle \rho_M(\mathbf{k}, t) \rho_M(-\mathbf{k}, 0) \rangle . \quad (6)$$

Then partial dynamic structure factors are calculated by the numerical Fourier transformation of these functions, for example, as

$$S_{\text{LiLi}}(\mathbf{k}, \omega) = (2\pi)^{-1} \int F_{\text{LiLi}}(\mathbf{k}, t) \exp(-i\omega t) dt , \quad (7)$$

and the charge-charge and mass-mass dynamic structure factors are given by

$$S_{CC}(\mathbf{k}, \omega) = (2\pi)^{-1} \int F_{CC}(\mathbf{k}, t) \exp(-i\omega t) dt , \quad (8)$$

$$S_{MM}(\mathbf{k}, \omega) = (2\pi)^{-1} \int F_{MM}(\mathbf{k}, t) \exp(-i\omega t) dt . \quad (9)$$

Since, for isotropic liquids, these functions are independent of the direction of wave vector  $\mathbf{k}$  and depend only on the magnitude, they were averaged over all wave vectors having the same  $|\mathbf{k}|$  value. In the calculation, the wave number  $k = |\mathbf{k}|$  was given the discrete values,

$$\mathbf{k} = 2\pi(n_x, n_y, n_z)/L , \quad (10)$$

where  $n_x, n_y,$  and  $n_z$  are integers in accordance with the periodic nature of our MD systems. The selected  $k$  values were 0.3845, 0.6079, 0.8156, 1.0173, 1.1851, 1.4127, 1.6085, 1.9979, 2.1920, 2.9907, and 5.9814 Å<sup>-1</sup> for LiCl pure melt and 0.3736, 0.6101, 0.8071, 0.9884, 1.1814, 1.3979, 1.6141, 1.8046, 1.9886, 2.1997, 2.9965, and 5.9931 Å<sup>-1</sup> for LiCl-CsCl mixture melt.

Trajectory data were divided into 10 and 17 subsets without any overlap along time for pure and mixture melts, respectively, each of which consisted of 7 000 steps of ion trajectories at every 4 fs. Collective autocorrelation functions such as intermediate structure factors were calculated for each subset by taking each step as the time origin. The functions were averaged over all the time origins and all the wave vectors  $\mathbf{k}$  with the same wave number  $k = |\mathbf{k}|$ . The fluctuation of the calculated functions among these subsets was small. Each subset must be long enough to be statistically independent of each other because the duration time of the subset (28 ps) was so long that the correlation functions well converged to zero. The functions which appear in the following figures are

averaged over these subsets and presented only for the first 0.8 or 3.0 ps. One subset was long enough to obtain also the single-particle autocorrelation functions with sufficient statistics because these were averaged over hundreds of particles. Thus, velocity autocorrelation functions and mean-square displacements were evaluated from only one arbitrarily chosen subset of trajectories for pure and mixture melt. The sampling number was, for example, 701 250 for  $F(k, t)$  of mixture melt at  $t = 0.5$  ps and at  $k \approx 0.4 \text{ \AA}^{-1}$ , and 1 600 000 for  $[\Delta r(t)]^2$  of  $\text{Cl}^-$  ions at  $t = 3$  ps.

### III. RESULTS AND DISCUSSION

#### A. Single-particle motions

The mean-square displacement of the ions as a function of time is shown in Fig. 1(a) and 1(b) for pure LiCl and LiCl-CsCl mixture melts, respectively. The resulting self-diffusion coefficients  $D_S$  are  $9.39 \times 10^{-9}$  and  $6.52 \times 10^{-9} \text{ m}^2 \text{ s}^{-1}$  for  $\text{Li}^+$  and  $\text{Cl}^-$  ions in the pure melt, respectively, and  $2.33 \times 10^{-9}$ ,  $2.83 \times 10^{-9}$ , and  $3.07 \times 10^{-9} \text{ m}^2 \text{ s}^{-1}$  for  $\text{Li}^+$ ,  $\text{Cs}^+$ , and  $\text{Cl}^-$  ions in the mixture melt, respectively. It is clear that, in the pure salt, the  $D_S$  value of the  $\text{Li}^+$  ion is larger than that of the  $\text{Cl}^-$  ion. This can be easily understood as the mass difference of the ions, i.e.,  $1.15 \times 10^{-26}$  and  $5.89 \times 10^{-26} \text{ kg}$  for  $\text{Li}^+$  and  $\text{Cl}^-$ , respectively. In the mixture melt, however, the order is reversed. The  $D_S$  value of the  $\text{Li}^+$  ion in the mixture is considerably smaller than that of  $\text{Li}^+$  in the pure melt and still smaller than that of  $\text{Cs}^+$  in the mixture, which is the heaviest ion among the constituents, i.e.,  $22.07 \times 10^{-26} \text{ kg}$ . It is interesting that the translational motion of the  $\text{Li}^+$  ion is much less diffuse in

the mixture than in the pure melt. In fact, the first peak height of the partial radial distribution functions  $g_{\text{LiCl}}(r)$  from the present MD calculations in the mixture was 8.8, which is much higher than the value, 3.8, in the pure melt. This clearly reveals, from a structural point of view, that the  $\text{Li}^+$  ion is strongly localized around the counteranion, which supports the less-diffuse behavior of the  $\text{Li}^+$  ion. These suggestions correspond well with the ionic mobilities in the melts.<sup>36</sup>

Figure 2 presents the velocity autocorrelation functions  $z(t)$ . In each system, the value for  $\text{Li}^+$  ions exhibit marked oscillations in time, which must originate from the small mass of  $\text{Li}^+$  ions in combination with the large mass of  $\text{Cl}^-$  ions. Furthermore, the oscillation in the mixture possesses a larger amplitude and persists for a longer time than in the pure salt. This reveals that the translational motions of  $\text{Li}^+$  and  $\text{Cl}^-$  ions show a more oscillatory character, which may be closely related to the result that the self-diffusion coefficients of  $\text{Li}^+$  and  $\text{Cl}^-$  ions in the mixture are smaller than in the pure salt. The power spectra  $z(\omega)$  of the velocity autocorrelation function  $z(t)$  are presented in Fig. 3. In the pure salt, the frequency for the  $\text{Li}^+$  ion is distributed over a wide range, where two peaks appeared at about  $\omega = 252$  and  $409 \text{ cm}^{-1}$ . These two peaks represent two vibrational modes of the translational motion of  $\text{Li}^+$  ion, whose origin, however, is not clear in the present stage of this analysis. The function of the  $\text{Cl}^-$  ion consists of a prominent peak at  $\omega = 64 \text{ cm}^{-1}$ , which is considerably lower than those of the  $\text{Li}^+$  ion. The behavior of the spectra of these two ions is very different from each other, which implies that the libration of  $\text{Cl}^-$  ions of this frequency is not particularly correlated with that of  $\text{Li}^+$  ions. However, it must be noted that the long tail of the spectrum for the  $\text{Cl}^-$  ion is found in the higher-frequency region, i.e.,  $300\text{--}500 \text{ cm}^{-1}$ , which represents some, although very small, correlation with the motion of the  $\text{Li}^+$  ion.

With regard to  $z(\omega)$  of the  $\text{Li}^+$  ion in the mixture, the distribution at the lower frequencies, i.e.,  $0\text{--}200 \text{ cm}^{-1}$ ,

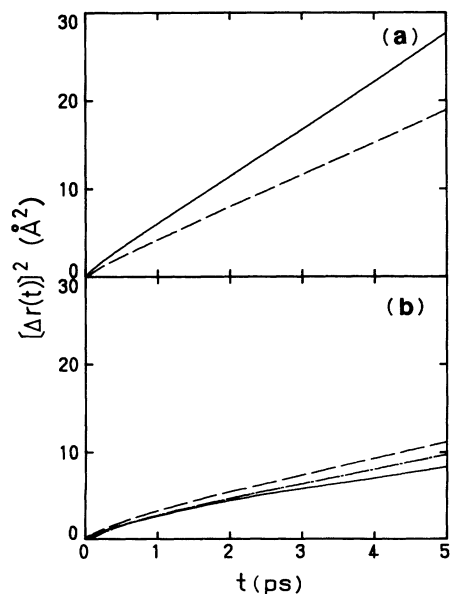


FIG. 1. Mean-square displacement  $[\Delta r(t)]^2$  for  $\text{Li}^+$  (—),  $\text{Cl}^-$  (---), and  $\text{Cs}^+$  (-·-·-) ions in (a) pure LiCl melt and (b) LiCl-CsCl mixture melt.

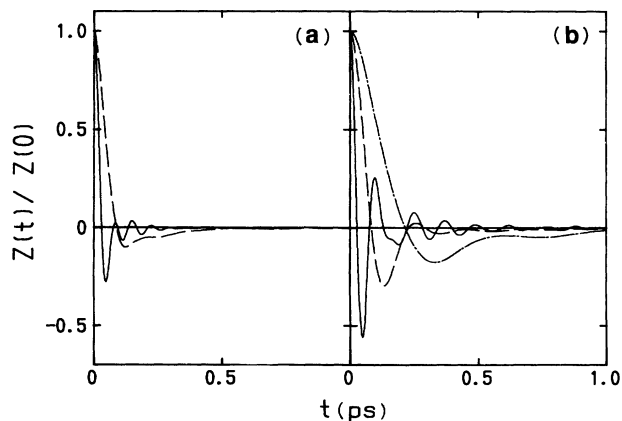


FIG. 2. Velocity autocorrelation function  $z(t)$  for  $\text{Li}^+$  (—),  $\text{Cl}^-$  (---), and  $\text{Cs}^+$  (-·-·-) ions in (a) pure LiCl melt and (b) LiCl-CsCl mixture melt.

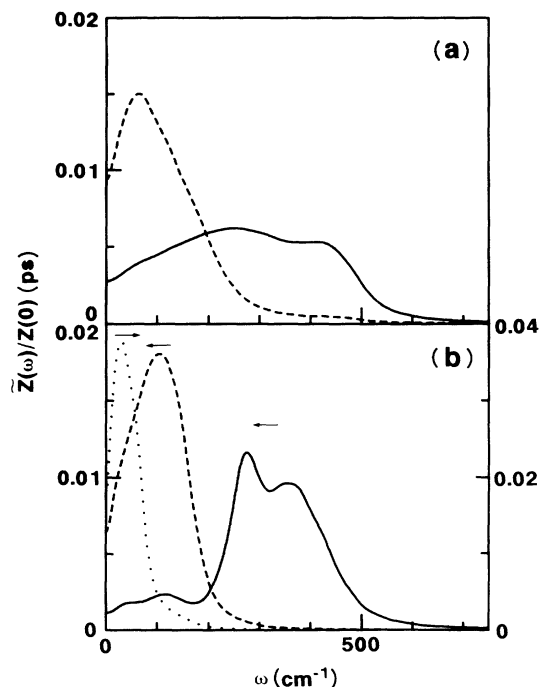


FIG. 3. Power spectrum  $z(\omega)$  of velocity autocorrelation function for  $\text{Li}^+$  (—),  $\text{Cl}^-$  (---), and  $\text{Cs}^+$  (-·-·-) ions in (a) pure LiCl melt and (b) LiCl-CsCl mixture melt.

decreases compared with that in the pure salt, while the distribution at higher frequencies, i.e., 200–450  $\text{cm}^{-1}$ , increases, resulting in the more pronounced peaks at  $\omega=276$  and 353  $\text{cm}^{-1}$ . The difference in the two peak positions is smaller in the mixture. The high-frequency tail for the  $\text{Cl}^-$  ion diminishes to some extent in the mixture, where the concentration of  $\text{Li}^+$  ions is small. This suggests that the tail represents the correlated motion of  $\text{Cl}^-$  ions with  $\text{Li}^+$  ions.

### B. Intermediate structure factors

The intermediate structure factors  $F_{CC}(k,t)$  and  $F_{MM}(k,t)$  of the pure LiCl melt are presented in Fig. 4 for selected  $k$  values. Remarkable oscillation is found for  $F_{CC}(k,t)$  at small  $k$ , the period of which becomes longer with increasing  $k$ . This implies the presence of a longitudinal optic (LO) mode in this melt. LO modes in charge-charge density fluctuation have already been found widely in other systems mainly by MD calculations<sup>16–20</sup> and will be discussed in detail in the following subsection. The oscillatory character diminishes with increasing  $k$  values and entirely disappears when  $k \geq 1.6 \text{ \AA}^{-1}$ , followed by a smooth exponential-like decay whose rate decreases as  $k$  increases to 2.0  $\text{\AA}^{-1}$ , and then increases. The minimum rate corresponds to the first peak position in the static structure factor  $S(k)$ . This phenomenon in the time domain corresponds to the de Gennes narrowing found in the frequency domain.<sup>37</sup>

On the other hand,  $F_{MM}(k,t)$  shows considerably different behavior. It decays smoothly and the rate as a function of  $k$  clearly shows the same de Gennes narrow-

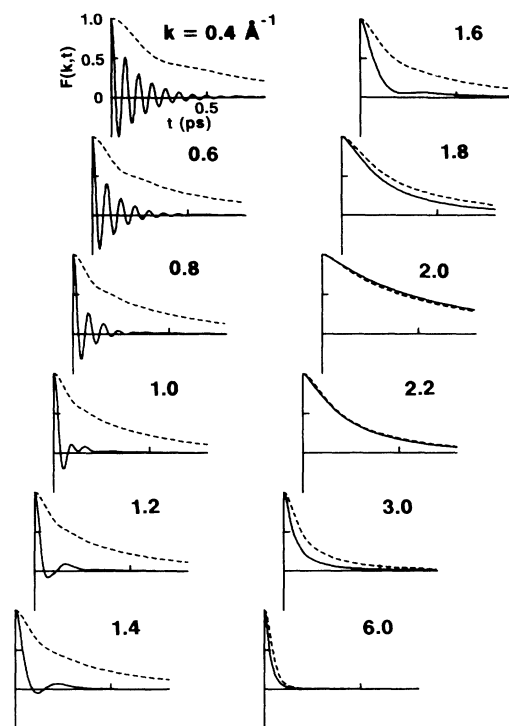


FIG. 4. Charge-charge (—) and mass-mass (---) intermediate structure factors  $F_{CC}(k,t)$  and  $F_{MM}(k,t)$ , respectively, as a function of  $t$  at selected wave numbers  $k$  for pure LiCl melt.

ing. However, it is noteworthy that some oscillation with very small amplitude is superimposed on the exponential-like decay, being clearly observed for  $k \approx 0.4$ , 0.6 and 0.8  $\text{\AA}^{-1}$  with the frequency becoming larger with increasing  $k$ . This indicates an acoustic-type dispersion, a longitudinal acoustic (LA) mode in the mass-mass density fluctuation. A phonon of this type has not hitherto been reported in other molten alkali halide systems. This may arise because the mass as well as the size of the  $\text{Li}^+$  ion is considerably smaller than the other ions studied so far. The oscillation is, however, no longer detectable even at  $k \geq 1.0 \text{ \AA}^{-1}$ , long before reaching 2.0  $\text{\AA}^{-1}$ , which corresponds to the nearest-neighbor distance. This contrasts with LA mode in one-component plasmas.<sup>15</sup>

The number density fluctuation of the  $\text{Li}^+$  ion,  $F_{\text{LiLi}}(k,t)$ , presented in Fig. 5, shows a qualitatively similar behavior to that of  $F_{MM}(k,t)$ . A very small oscillation was found on the exponential-like decay when  $k \leq 1.2 \text{ \AA}^{-1}$ , although it disappeared for larger  $k$  values. The period of the oscillation, however, is considerably shorter than that of  $F_{MM}(k,t)$  and almost the same as  $F_{CC}(k,t)$ .

For the LiCl-CsCl melt, the number density autocorrelation functions of the  $\text{Li}^+$  ion  $F_{\text{LiLi}}(k,t)$  are also shown in Fig. 5, and the charge-charge and mass-mass density autocorrelation functions  $F_{CC}(k,t)$  and  $F_{MM}(k,t)$ , respectively, in Fig. 6. These functions for the mixture are similar to those for the pure melt, but with two remarkable differences in the  $F_{CC}(k,t)$ 's at small  $k$ . The first is concerned with the oscillatory character, for which a

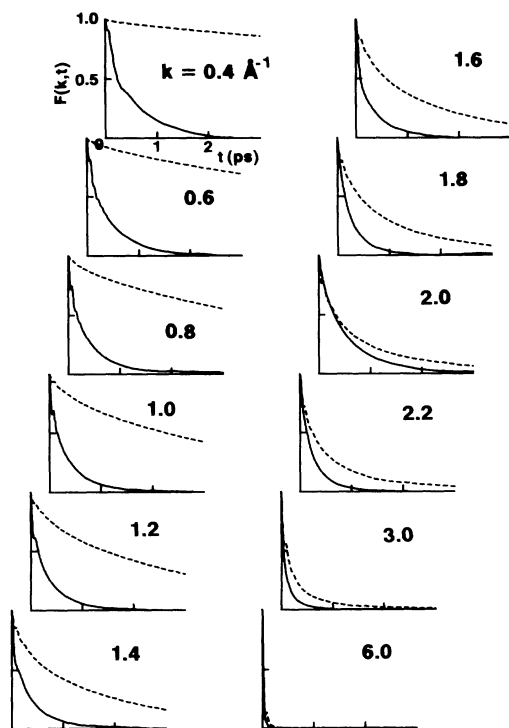


FIG. 5. Intermediate partial structure factor  $F_{\text{LiLi}}(k, t)$  as a function of  $t$  at selected wave numbers  $k$  for pure LiCl melt (—) and LiCl-CsCl mixture melt (---).

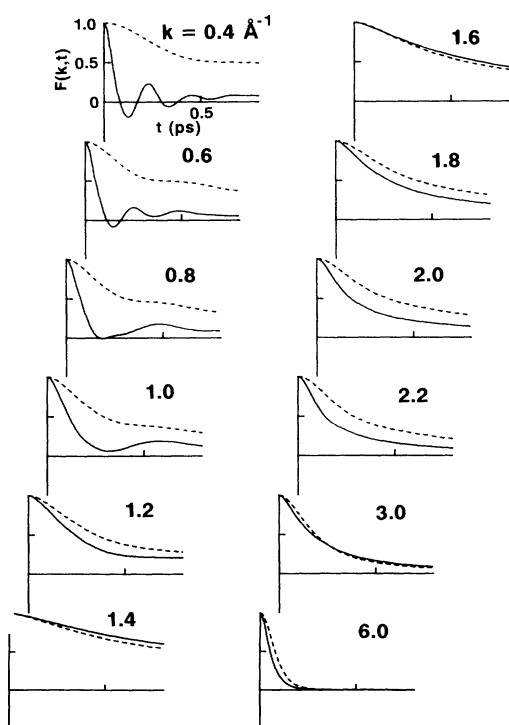


FIG. 6. Charge-charge (—) and mass-mass (---) intermediate structure factors  $F_{\text{CC}}(k, t)$  and  $F_{\text{MM}}(k, t)$ , respectively, as a function of  $t$  at selected wave numbers  $k$  for LiCl-CsCl mixture melt.

much longer period and a smaller amplitude were observed. The other is the slowly converging smooth decay which forms a baseline of the oscillation. The function for the mixture possesses a long tail even at small  $k$  values, while that for the pure melt converges strongly, oscillating around the zero value, and are discussed later.

With regard to the number density autocorrelation functions, both  $F_{\text{ClCl}}(k, t)$  and  $F_{\text{CsCs}}(k, t)$  show a similar behavior to  $F_{\text{LiLi}}(k, t)$  in the pure salt and in the mixture: a steady decay with a small amplitude oscillation on it, the decay rate and oscillation frequency differing with the mass.

### C. Dynamic structure factors

The dynamic structure factors  $S(k, \omega)$  were evaluated from the numerical Fourier transformation of  $F(k, t)$ . Since the Riemann window was used to avoid a large truncation ripple caused by the slow convergence of  $F(k, t)$ , some artificial broadening of the peaks could have occurred. However, it would not influence the peak positions of the spectra, presented in Figs. 7–9. In the pure LiCl salt (Fig. 7), when  $k \approx 0.4 \text{ \AA}^{-1}$ , only one intense peak was observed at  $\omega = 467 \text{ cm}^{-1}$ . With increasing  $k$ , this peak shifts toward the lower  $\omega$  and becomes broader, and merges into the quasielastic peak when  $k \approx 1.8 \text{ \AA}^{-1}$ . The peak position is plotted in Fig. 10, which clearly shows a negative dispersion, having a finite frequency of the limit  $k \rightarrow 0 \text{ \AA}^{-1}$ . Such an optic-type dispersion as this has been often reported in other papers

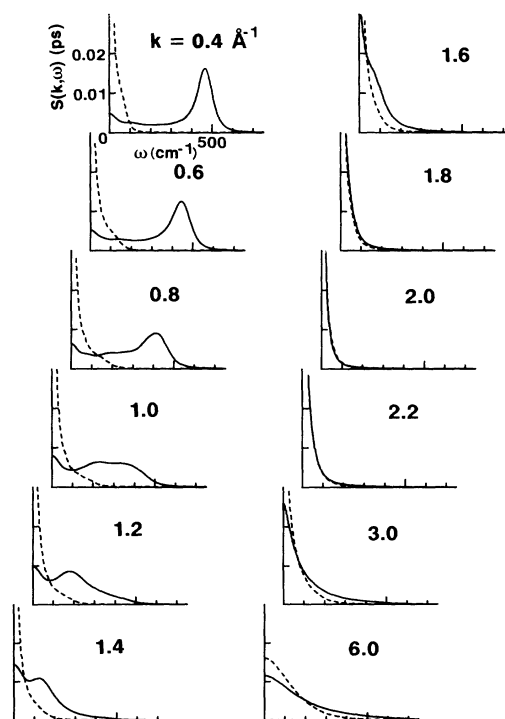


FIG. 7. Charge-charge (—) and mass-mass (---) structure factors  $S_{\text{CC}}(k, \omega)$  and  $S_{\text{MM}}(k, \omega)$ , respectively, as a function of  $\omega$  at selected wave numbers  $k$  for pure LiCl melt.

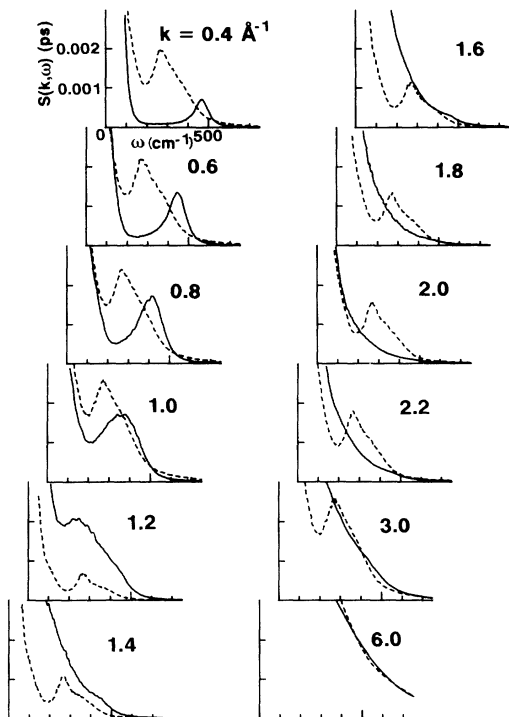


FIG. 8. Partial structure factor  $S_{\text{LiLi}}(k, \omega)$  as a function of  $\omega$  at selected wave numbers  $k$  for pure LiCl melt (—) and LiCl-CsCl mixture melt (---).

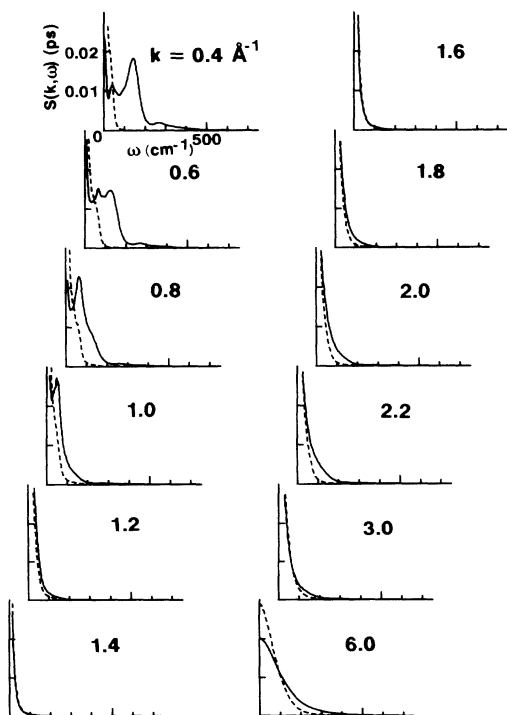


FIG. 9. Charge-charge (—) and mass-mass (---) structure factors  $S_{\text{CC}}(k, \omega)$  and  $S_{\text{MM}}(k, \omega)$ , respectively, as a function of  $\omega$  at selected wave numbers  $k$  for LiCl-CsCl mixture melt.

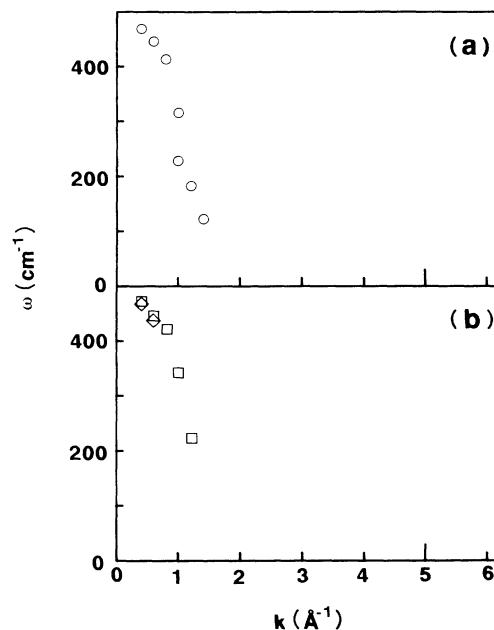


FIG. 10. Dispersion curve for (a) charge-charge density fluctuation and (b) number density fluctuations in pure LiCl melt.  $\circ$ :  $S_{\text{CC}}(k, \omega)$ ,  $\square$ :  $S_{\text{LiLi}}(k, \omega)$ , and  $\diamond$ :  $S_{\text{ClCl}}(k, \omega)$ .

on MD simulations of molten salts.<sup>16–20</sup> However, it is remarkable that two distinct peaks were found at  $\omega = 225$  and  $313 \text{ cm}^{-1}$  when  $k \approx 1.0 \text{ \AA}^{-1}$  as shown in Fig. 7 and that, at the same time, two lines can be drawn for the dispersion plot of  $S_{\text{CC}}(k, \omega)$  in Fig. 10. These reveal that two different types of LO modes coexist in the pure melt, one of which propagates over the range of small wave numbers, i.e.,  $0 \leq k \leq 1.0 \text{ \AA}^{-1}$  and the other over larger wave numbers, i.e.,  $k \geq 1.0 \text{ \AA}^{-1}$ . To our knowledge, no such observation has been previously reported either for neutral or charged particles. Furthermore, it is noteworthy that the frequency regions occupied by the two types of LO modes in  $S_{\text{CC}}(k, \omega)$  seem roughly to coincide with those of the two broad peaks in the spectrum  $z(\omega)$  of the velocity autocorrelation function of the  $\text{Li}^+$  ion. The collective motions represented by the two types of LO modes thus closely correlate with the single-particle motions of the  $\text{Li}^+$  ion.  $\text{Li}^+$  ions may, thus, belong to two different kinds of states in the liquid, in each of which the ions take both particular single-particle and collective motions.

In the dynamic structure factor  $S_{\text{MM}}(k, \omega)$  for the pure melt, only one quasielastic peak at  $\omega = 0 \text{ cm}^{-1}$  was clear for all  $k$  values, de Gennes narrowing being found with a minimum width at  $k \approx 2.0 \text{ \AA}^{-1}$ . In the frequency domain, however, the Brillouin peak, which corresponds to the very small oscillation in  $F_{\text{MM}}(k, t)$  in Fig. 4, was not distinct, though a very small shoulder was just detected, at several tens  $\text{cm}^{-1}$ , when  $k \approx 0.4 \text{ \AA}^{-1}$ .

The partial dynamic structure factor  $S_{\text{LiLi}}(k, \omega)$ , shown in Fig. 8, has a strong quasielastic peak at  $\omega = 0 \text{ cm}^{-1}$  as well as a very weak Brillouin peak at several hundred  $\text{cm}^{-1}$  in accord with the intermediate structure factor

$F_{\text{LiLi}}(k, t)$ , the intensity of the Brillouin peak being one order of magnitude smaller than that of  $S_{\text{CC}}(k, \omega)$ . As shown in Fig. 10(b), the Brillouin peak in  $S_{\text{LiLi}}(k, \omega)$  shows a negative dispersion, which is also the case with the  $S_{\text{ClCl}}(k, \omega)$ . It should be pointed out that the dispersion relation of  $S_{\text{LiLi}}(k, \omega)$  and  $S_{\text{ClCl}}(k, \omega)$  resembles that of  $S_{\text{CC}}(k, \omega)$  rather than that of  $S_{\text{MM}}(k, \omega)$ . However, the physical reason for this is not clear at present, although the difference in the phonon phase may be related.

On the other hand, in the mixture,  $S_{\text{CC}}(k, \omega)$  shows a more complicated behavior than in the pure melt, as shown in Fig. 9. For small wave numbers  $k$ , there exist three distinct Brillouin peaks in addition to a comparatively intense quasielastic peak at  $\omega = 0 \text{ cm}^{-1}$ . At  $k \approx 0.4 \text{ \AA}^{-1}$ , of the three modes, the lowest and highest are considerably weaker than the intermediate one. As shown in Fig. 11(a), the highest-frequency peak shows a slightly negative dispersion, the intermediate a relatively strong negative one, and the lowest an apparent maximum. The first mode persists over a wide range of  $k$ , while the second disappears when  $k \geq 1.0 \text{ \AA}^{-1}$ , and the last is absorbed by the large quasielastic peak when  $k \approx 1.2 \text{ \AA}^{-1}$ . In contrast to the case of the pure melt, the frequency regions of these three modes are not exactly the same as the three peaks in the power spectrum of velocity autocorrelation function of  $\text{Li}^+$ . However, the behavior of  $S_{\text{MM}}(k, \omega)$  of the mixture is almost the same as the pure melt except for a more distinct shoulder in the former representing the longitudinal acoustic mode. The very weak Brillouin peak of  $S_{\text{LiLi}}(k, \omega)$  for the mixture, in Fig. 8, is interesting, since the dispersion curve shows a nearly zero slope line persisting over all the  $k$  regions examined, as shown in Fig. 11(b). The frequency is nearly the same with that of the highest-frequency peak in  $S_{\text{CC}}(k, \omega)$ . This suggests that at least one of the LO modes in the charge-charge density fluctuation may be caused by the collective motion of  $\text{Li}^+$  ions. The frequencies also coincide with that of the most intense peak in the spectrum of the velocity autocorrelation function of the  $\text{Li}^+$  ion, which reveals a close correlation between the collective motion of the liquid and the single-particle motion in it.

#### IV. CONCLUSION

Phonon propagation was found both in charge-charge and mass-mass density fluctuations in ionic melts which consist of light, small ions and heavy, large ions. The former phonon mode showed an optic-type dispersion relation, and the latter, an acoustic type. The presence of an acoustic mode in  $S_{\text{MM}}(k, \omega)$  in alkali halide melts has

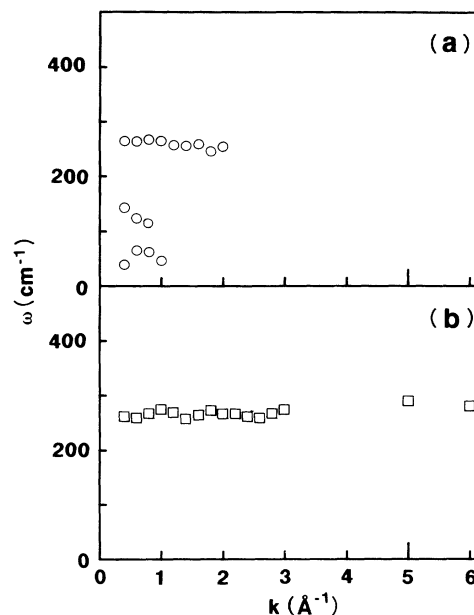


FIG. 11. Dispersion curve for (a) charge-charge density fluctuation and (b) number density fluctuation in LiCl-CsCl mixture melt.  $\circ$ :  $S_{\text{CC}}(k, \omega)$  and  $\square$ :  $S_{\text{LiLi}}(k, \omega)$ .

been successfully demonstrated by MD calculations; this mode may be related to the presence of small, light  $\text{Li}^+$  ions. A more remarkable finding is that two different phonon modes certainly exist in  $S_{\text{CC}}(k, \omega)$  in the pure LiCl melt and three in the LiCl-CsCl melt. Such phonons have not been found in the other ionic systems studied to date. This phenomenon seems to be caused by the combination of small, light ions with large, heavy ions. The collective motions of the melts were found to correlate closely with the single-particle motions, in particular, those of  $\text{Li}^+$  ions in the melts.

#### ACKNOWLEDGMENTS

The authors thank the Computer Center of the Institute for Molecular Science and High Energy Physics Institute for the use of the HITAC S-820 and M-680H computers. We acknowledge gratefully partial support of this work by a Grant-in-Aid for Scientific Research (No. 03854044) and a Grant-in-Aid for Scientific Research on Priority Area of "Molecular Approaches to Non-equilibrium Process in Solutions" (No. 03231103) from the Ministry of Education, Science and Culture, Japan.

<sup>1</sup>D. Levesque, L. Verlet, and J. Kurkijarvi, Phys. Rev. A **7**, 1690 (1973).

<sup>2</sup>A. Rahman, Phys. Rev. Lett. **32**, 52 (1974).

<sup>3</sup>A. Rahman, Phys. Rev. A **9**, 1667 (1974).

<sup>4</sup>J. J. Weis and D. Levesque, Phys. Rev. A **13**, 450 (1976).

<sup>5</sup>M. Schoen and C. Hoheisel, Mol. Phys. **58**, 181 (1986).

<sup>6</sup>J. Bosse, G. Jacucci, M. Ronchetti, and W. Schirmacher, Phys. Rev. Lett. **57**, 3277 (1986).

<sup>7</sup>N. Ohtomo and Y. Tanaka, J. Phys. Soc. Jpn. **56**, 2801 (1987).

<sup>8</sup>M. A. Ricci, D. Rocca, and R. Vallauri, Phys. Rev. A **40**, 7226 (1989).

<sup>9</sup>B. Dorner, T. Plesser, and H. Stiller, Discuss. Faraday Soc. **43**, 160 (1967).

<sup>10</sup>K. Carneiro, M. Nielsen, and J. P. McTague, Phys. Rev. Lett. **30**, 481 (1973).

<sup>11</sup>J. R. D. Copley and J. M. Rowe, Phys. Rev. Lett. **32**, 49

- (1974).
- <sup>12</sup>A. A. van Well, P. Verkerk, L. A. de Graaf, J.-B. Suck, and J. R. D. Copley, *Phys. Rev. A* **31**, 3391 (1985).
- <sup>13</sup>T. Gaskell, *J. Phys. F* **16**, 381 (1986).
- <sup>14</sup>M. A. Ricci, G. Ruocco, D. Rocca, and R. Vallauri, *Helv. Phys. Acta* **62**, 676 (1989).
- <sup>15</sup>J. P. Hansen, I. R. McDonald, and E. L. Pollock, *Phys. Rev. A* **11**, 1025 (1975).
- <sup>16</sup>J. P. Hansen and I. R. McDonald, *Phys. Rev. A* **11**, 2111 (1975).
- <sup>17</sup>J. R. Copley and A. Rahman, *Phys. Rev. A* **13**, 2276 (1976).
- <sup>18</sup>E. M. Adams, I. R. McDonald, and K. Singer, *Proc. R. Soc. London, Ser. A* **357**, 37 (1977).
- <sup>19</sup>S. W. de Leeuw, *Mol. Phys.* **37**, 489 (1979).
- <sup>20</sup>M. Dixon, *Philos. Mag. B* **47**, 531 (1983).
- <sup>21</sup>J. R. D. Copley and G. Dolling, *J. Phys. C* **11**, 1259 (1978).
- <sup>22</sup>R. L. McGreevy and E. W. J. Mitchell, *J. Phys. C* **15**, L1001 (1982).
- <sup>23</sup>R. L. McGreevy, E. W. Mitchell, and F. M. A. Margaca, *J. Phys. C* **17**, 775 (1984).
- <sup>24</sup>F. M. A. Margaca, R. L. McGreevy, and E. W. Mitchell, *J. Phys. C* **17**, 4725 (1984).
- <sup>25</sup>R. L. McGreevy and E. W. J. Mitchell, *J. Phys. C* **18**, 1163 (1985).
- <sup>26</sup>R. L. McGreevy, E. W. J. Mitchell, F. M. A. Margaca, and M. A. Howe, *J. Phys. C* **18**, 5235 (1985).
- <sup>27</sup>L. Pusztai and R. L. McGreevy, *J. Phys. Condens. Matter* **1**, 2369 (1989).
- <sup>28</sup>Y. Kaneko and A. Ueda, *Phys. Rev. B* **39**, 10 281 (1989).
- <sup>29</sup>G. Eckold, K. Funke, J. Kalus, and R. E. Lechner, *J. Phys. Chem. Solids* **37**, 1097 (1976).
- <sup>30</sup>I. Okada, *Z. Naturforsch. Teil A* **42**, 21 (1987).
- <sup>31</sup>F. Lantelme and P. Turq, *J. Chem. Phys.* **77**, 3177 (1982).
- <sup>32</sup>G. J. Janz, R. P. T. Tomkins, C. B. Allen, J. R. Downey, Jr., G. L. Gardner, U. Krebs, and S. K. Singer, *J. Phys. Chem. Ref. Data* **4**, 871 (1975).
- <sup>33</sup>M. P. Tosi and F. G. Fumi, *J. Phys. Chem. Solids* **25**, 45 (1964).
- <sup>34</sup>M. Dixon and M. J. Gillan, *Philos. Mag. B* **43**, 1099 (1981).
- <sup>35</sup>B. Larsen, T. Førland, and K. Singer, *Mol. Phys.* **26**, 1521 (1973).
- <sup>36</sup>M. Chemla and I. Okada, *Electrochim. Acta* **35**, 1761 (1990).
- <sup>37</sup>P. G. de Gennes, *Physica* **25**, 825 (1959).